J. Dairy Sci. 107:2681–2689
https://doi.org/10.3168/jds.2023-23481

Detection of carbon nanotubes in bovine raw milk through Fourier transform Raman spectroscopy

Philipe P. Nunes,[1] Mariana R. Almeida,[2] Flávia G. Pacheco,[3] Cristiano Fantini,[4] Clascídia A. Furtado,[3] Luiz O. Ladeira,[4] Ado Jorio,[4] Antônio P. M. Júnior,[1] Renato L. Santos,[1] and Álan M. Borges[1]*

[1]Department of Veterinary Clinic and Surgery, Veterinary School, Federal University of Minas Gerais, Belo Horizonte, MG 31270-901, Brazil
[2]Department of Chemistry, Institute of Exact Science, Federal University of Minas Gerais, Belo Horizonte, MG 31270-901, Brazil
[3]Laboratory of Carbon Nanostructure Chemistry, Nuclear Technology Development Center, Belo Horizonte, MG 31270-901, Brazil
[4]Department of Physics, Institute of Exact Science, Federal University of Minas Gerais, Belo Horizonte, MG 31270-901, Brazil

ABSTRACT

The potential use of carbon-based methodologies for drug delivery and reproductive biology in cows raises concerns about residues in milk and food safety. This study aimed to assess the potential of Fourier transform Raman spectroscopy and discriminant analysis using partial least squares (PLS-DA) to detect functionalized multiwalled carbon nanotubes (MWCNT) in bovine raw milk. Oxidized MWCNT were diluted in milk at different concentrations from 25.00 to 0.01 μg/mL. Raman spectroscopy measurements and PLS-DA were performed to identify low concentrations of MWCNT in milk samples. The PLS-DA model was characterized by the analysis of the variable importance in projection (VIP) scores. All the training samples were correctly classified by the model, resulting in no false-positive or false-negative classifications. For test samples, only one false-negative result was observed, for 0.01 μg/mL MWCNT dilution. The association between Raman spectroscopy and PLS-DA was able to identify MWCNT diluted in milk samples up to 0.1 μg/mL. The PLS-DA model was built and validated using a set of test samples and spectrally interpreted based on the highest VIP scores. This allowed the identification of the vibrational modes associated with the D and G bands of MWCNT, as well as the milk bands, which were the most important variables in this analysis.
Key words: carbon nanotube, cow, milk, partial least squares-discriminant analysis, Raman spectroscopy

INTRODUCTION

Carbon nanotubes (**CNT**) are carbon-based nanostructures composed of one or more concentrically rolled graphene sheets, with diameter ranging at the nanometer scale and length achieving few micrometers (Ijima, 1991). Because of its relatively high surface area and the possibility to add functional groups over its surface, CNT can be solubilized in water and can easily interact with other biological molecules. Functionalized CNT can be employed in many fields of science as biosensor or for tissue engineering, drug delivery, cancer treatment, and gene therapy (Liu et al., 2008; Varkouhi et al., 2011; Shimizu et al., 2012). Therefore, CNT represent an interesting alternative to improve diagnostic systems (Pourasl et al., 2014; Lee et al., 2018), regenerative medicine (Newman et al., 2013; Lekshmi et al., 2020), and conventional vectors for drug delivery in humans and animals (Liu et al., 2008; Ladeira et al., 2010). Carbon nanotubes have been employed as transfection reagents for small interfering RNA into mice and human cell lines for in vitro gene silencing (Ladeira et al., 2010; Apartsin et al., 2014). In the reproductive biology field, nanomaterials, and CNT have been employed in chronic disease treatment (Chaudhury et al., 2013), support for assisted reproduction techniques (Barkalina et al., 2014), and bovine embryogenesis (Munk et al., 2016).

However, the application of CNT-based methodologies in farm animals, especially in dairy cows, raises concerns about food safety, as milk represents an excretion route for drug residues in lactating cows. Currently, one of the major problems faced worldwide by the dairy industry is the detection of drug residue in raw milk, due to the indiscriminate use of antibiotics and other drugs in dairy herds without veterinary assistance and with no respect to the withholding period (Bando et al., 2009; Redding et al., 2014; Tempini et al., 2018). This behavior is associated with the increasing microbial resistance to antibiotics, which directly affects animal and human health (Chen et al., 2019).

Studies evaluating the in vivo pharmacokinetics of functionalized CNT (Ali-Boucetta and Kostarelos, 2013; Rodriguez-Yañez et al., 2013; Jacobsen et al., 2017) demonstrated that nanotubes injected intrave-

Received March 12, 2023.
Accepted October 11, 2023.
*Corresponding author: alanmborges@hotmail.com

nously in mice accumulated mainly in the liver and spleen, with lesser amounts in the lungs and kidneys, followed by a high excretion through urine. By intraperitoneal route, functionalized CNT accumulated in the stomach, kidneys, bones, blood, spleen, and liver. Oral administration of functionalized CNT in rats resulted in accumulation in the stomach and upper and lower intestines, with higher excretion through feces (Ali-Boucetta and Kostarelos, 2013; Rodriguez-Yañez et al., 2013; Jacobsen et al., 2017). Studies with in vitro cell culture using human and mice cell lines demonstrated some cytotoxic effect when CNT were used in higher concentrations (5–10 mg/mL; Pantarotto et al., 2004; Bianco et al., 2005), whereas smaller concentrations (20–100 μg/mL) had no significant cell damage or toxicity (Singh et al., 2006; Bottini et al., 2006; Firme and Bandaru, 2010). To our knowledge, no study has been conducted to assess the accumulation of functionalized CNT in udder and its elimination through milk.

Fourier transform Raman spectroscopy (**FT-Raman**) was used in in vitro studies to assess the nanotube toxicity in mice and zebrafish embryos (Dal Bosco et al., 2015; Girardi et al., 2017). The spectral signature of carbon nanotubes can be directly observed inside the tissues, and toxicological effects have been investigated regarding the nanotubes biodistribution. In the field of milk safety, recent studies used FT-Raman allied to chemometrics tools to analyze milk quality and detect the presence of adulterants such as whey and starch (Almeida et al., 2012; Mazurek et al., 2015; Rodrigues Júnior et al., 2016). Raman spectroscopy is based on the detection of electromagnetic energy that is inelastically scattered by molecular vibrations after excitation by a laser. It is a fast analytical tool that accesses the vibrational characteristics of molecules and discriminates, in complex samples, more than one organic and inorganic component at the same time, without previous sample preparation or sample destruction (Almeida et al., 2011; El-Abassy et al., 2011).The association between Raman spectroscopy and the supervised method partial least squares for discriminant analysis (**PLS-DA**) showed a high potential for use in the dairy industry for quality assessment of the main nutrients (fats, proteins, and carbohydrates) and the detection of adulterants in dairy products (de Sá Oliveira et al., 2016; Rodrigues Júnior et al., 2016; Genis et al., 2021).

The growing application of nanotechnologies in disease therapy and food technology raises a worldwide concern about biocompatibility, toxicity, food safety, and residual contamination with nanoparticles. In the literature, studies developed analytical methodologies for detection of carbon nanotubes in plant tissues. Das et al. (2018a) developed a digestion method coupled with programmed thermal analysis to quantify multiwalled carbon nanotubes (**MWCNT**) in lettuce tissues. The methodology presented a detection limit equal to 64.9 μg of CNT-bound carbon per gram of plant tissues. The same research group (Das et al., 2018b) proposed the use of the digestion method coupled with Raman spectroscopy, and the authors were able to detect functionalized MWCNT in lettuce leaves grown with 5, 10, and 20 mg/L of the nanomaterial.

The increasing use of nanomaterials in veterinary medicine and the lack of research focused on unraveling the pharmacokinetics and toxicity of CNT in livestock animals have turned the application of CNT in dairy cows into a point of concern and an important issue in food safety. To our knowledge, this is the first exploratory study that aimed to develop an alternative fast and inexpensive screening methodology using FT-Raman combined with a chemometric tool for detection of MWCNT in bovine raw milk. Accordingly, the goal of this study was to assess the potential of FT-Raman spectroscopy and PLS-DA method to detect functionalized MWCNT in bovine raw milk. The developed model was validated with an independent test set and the estimation of appropriate figures of merit. In addition, we developed a quantitative model employing partial least square (**PLS**) regression to show the potentiality of Raman spectroscopy in detecting and quantifying MWCNT in raw milk samples.

MATERIALS AND METHODS

All experimental procedures were previously approved by the Ethics Committee on the Use of Animals at the Federal University of Minas Gerais (CEUA-UFMG) under protocol number 409/2018.

Multiwalled Carbon Nanotubes

The MWCNT were produced by chemical vapor deposition, and their dimensions ranged from 10 to 25 nm in diameter and 5 to 30 μm in length. Pristine MWCNT were functionalized by oxidation using reflux with nitric and sulfuric acids, and purified according to Pacheco et al. (2015), using ethyl alcohol. Then, nanotubes were diluted in deionized water at 1 mg/mL and submitted to sonication in a cold bath for 60 min, using an ultrasonic processor with tapered horn tip (Sonics and Materials Inc., Newtown, CT). Nanotubes were air-dried at 80°C overnight. Additional information about MWCNT characterization for experimental use is presented in Supplemental File S1 and Supplemental Figures S1–S4 (http://osf.io/s5eq6; Nunes, 2023).

Raman Spectra Acquisition on Raw Milk and MWCNT Dispersions in Milk Samples

To avoid interference from factors such as breed, genetics, nutrition, days in lactation, age, and mastitis on the percentage of fat, protein, and minerals in milk (Linn, 1988), standardized raw milk samples were harvested from 3 crossbred (3/4 Holstein × 1/4 Zebu) cows at 65 to 92 DIM, with an average yield of 29.04 kg. Cows were maintained at a dairy farm in Minas Gerais province, under the same health and nutrition management. The selected animals had no clinical signs of udder inflammation and were not under recombinant bovine somatotropin treatment. Milk samples were harvested within a period of 21 d, one sample per week. Oxidized MWCNT (1.00 mg/mL) were dispersed in all milk samples, at 9 different concentrations, namely 25.00, 20.00, 15.00, 10.00, 7.50, 5.00, 1.0, 0.10, and 0.01 μg/mL. These concentrations were chosen according to in vitro studies assessing transfection efficiency of nanotubes over a mammal's cell lines (Ladeira et al., 2010) and concentrations associated with minimal or no toxic effect (Firme and Bandaru, 2010). Raw milk and MWCNT dispersed in milk samples were aliquoted in 2-mL glass vials and sonicated in ultrasonic bath for 10 min. Before analysis, samples were homogenized for 1 min by inversion and 15 s by gentle vortex. The macroscopic aspect of milk solutions was observed just before and after Raman spectra acquisition to evaluate phase segregation. Raman spectra of the samples were collected on a Vertex 70 spectrometer coupled to a FT-Raman module with a liquid nitrogen germanium detector and 1,064-nm Nd:YAG laser (Bruker). Laser excitation light (1,000 mW) was introduced and focused on the sample, and the backscattered radiation was collected. The spectrum was collected after 1,000 scans and with a resolution of 4 cm^{-1} over the range of 500 to 3,100 cm^{-1}. Raman spectrum of isopropanol was acquired as analytical standard. The software OPUS (Bruker) was used for FT-Raman data acquisition and spectral preprocessing.

Data Analysis

To identify the presence of low concentrations of MWCNT dispersed in milk samples, PLS-DA was performed. The discriminant analysis method was selected for classification in this study due to the nature of the samples and the high variance of control samples (Nunes et al., 2020).

The PLS-DA is based on PLS regression, which correlates independent spectral variables (**X** matrix) with a vector of dependent dummy variables (**Y** vector). The PLS-DA model was built using MATLAB version 8.4 (MathWorks, Natick) and PLS Toolbox version 7.0 (Eigenvector Technologies, Manson). A dummy vector **Y** was created with 0 and 1 representing bovine raw milk samples (control milk) and milk-dispersed MWCNT samples, respectively. Because PLS-DA provides predicted **Y** values that are not exactly 0 or 1, a Bayesian threshold was calculated.

The Raman spectra were preprocessed using the standard normal variate method for the correction of baseline deviations. Savitzky–Golay smoothing, with a window of 9 points, and mean centering were also performed. The spectral data matrix was split into 28 samples (12 bovine raw milk and 16 MWCNT dispersed in milk) for the training set and 17 samples (7 bovine raw milk and 10 MWCNT dispersed in milk) for the test set. This was done using the Kennard and Stone algorithm (Kennard and Stone, 1969) The concentration of MWCNT in milk ranged from 0.01 to 25.00 μg/mL. The training set was used to build the model, whereas the test set assessed its performance. The number of latent variables (**LV**) was selected using Venetian blinds cross-validation with 5 splits, based on the smallest cross-validation classification error. The performance of PLS-DA model was evaluated using the parameters of sensitivity, specificity, and efficiency. Sensitivity is the ability of a model to detect truly positive samples as positive (MWCNT positive). Specificity is the ability of a method to detect truly negative samples as negative (MWCNT negative), and efficiency is a global figure of merit that is estimated as the difference between the sum of results (100%) and the sum of false-positive and false-negative rates. Table 1 presents the equations used to calculate the figures of merit.

The PLS-DA model was characterized by analyzing the variable importance in projection (**VIP**) scores. The VIP scores indicate the significance of specific variables in the discriminant ability of the model. When the VIP value is greater than one, the variable is considered important in distinguishing a positive sample from a negative one.

For constructing the PLS model, 27 samples were used, 3 samples of milk without the addition of MWCNT, and 24 samples with MWCNT dispersed in the concentration range of 0.01 to 25.00 μg/mL. Samples were manually divided into calibration and validation sets. For the calibration samples, milk and MWCNT diluted in milk samples, corresponding to the entire spectral range of 0.00 to 25.00 μg/mL, were selected. The preprocessing was the same used in the PLS-DA model. The optimum number of LV was chosen by the root mean square error of cross-validation (**RMSECV**) obtained from the calibration set by internal validation (random subsets method). The performance of the models was evaluated by the root mean square

Table 1. Description of the performance parameters and their estimates for evaluating the partial least squares for discriminant analysis model[1]

Parameter	Equation	Training set (%)	Test set (%)
Sensitivity	$\frac{TP}{TP+FN}$	100	90
False-negative rate	$\frac{FN}{TP+FN}$	0	10
Selectivity	$\frac{TN}{TN+FP}$	100	100
False-positive rate	$\frac{FP}{TN+FP}$	0	0
Efficiency	$\frac{TN+TP}{TN+FP+TP+FN}$	100	90

[1]TP = true positive; TN = true negative; FP = false positive; FN = false negative.

error of calibration (**RMSEC**), root mean square error of prediction (**RMSEP**), and residual prediction deviation (**RPD**). The characterization of the model was done through the analysis of the VIP scores.

RESULTS AND DISCUSSION

Immediately after removing the milk samples from spectrometer, no phase segregation such as the supernatant milk fat ring was observed in any of the samples evaluated, indicating macroscopic stability during measurement. Raman spectra for raw milk and milk containing MWCNT dilutions from 25.00 to 0.01 µg/mL are presented in Figure 1. The Raman spectrum for raw milk, has scattering bands at 2,931, 2,856, 1,655, 1,450, 1,261, 1,122, 1,084, and 1,003 cm^{-1}. For milk samples with MWCNT, the Raman spectra have scattering bands at 2,931, 2,856, 1,450, 1,122, 1,084, and 1,003 cm^{-1}, and they are similar to those observed in milk spectrum. Scattering bands at 1,605 and 1,286 cm^{-1} presented high intensities in the lower nanotube dilution in milk, whereas signals decreased as the nanotube dilution increases. These 2 bands are associated, respectively, with the G and D bands of MWCNT, and their presence in the spectrum is clearly related to the presence of standardized MWCNT dispersed in the milk. Conversely, scattering band at 1,655 cm^{-1} presented a very small intensity in 25.00 µg/mL dilution, but its intensity increases as nanotube dilution also increases. The 1,655 cm^{-1} band is a well-established scattering band of milk spectrum associated with proteins and fatty acids (Almeida et al., 2011; El-Abassy et al., 2011; Rodrigues Júnior et al., 2016). When the dilution of MWCNT in milk is low, this band signal is suppressed by the high intensity signal of the G band. As the nanotube dilution in milk increases, the 1,655 cm^{-1} band signal becomes more evident in the Raman spectrum.

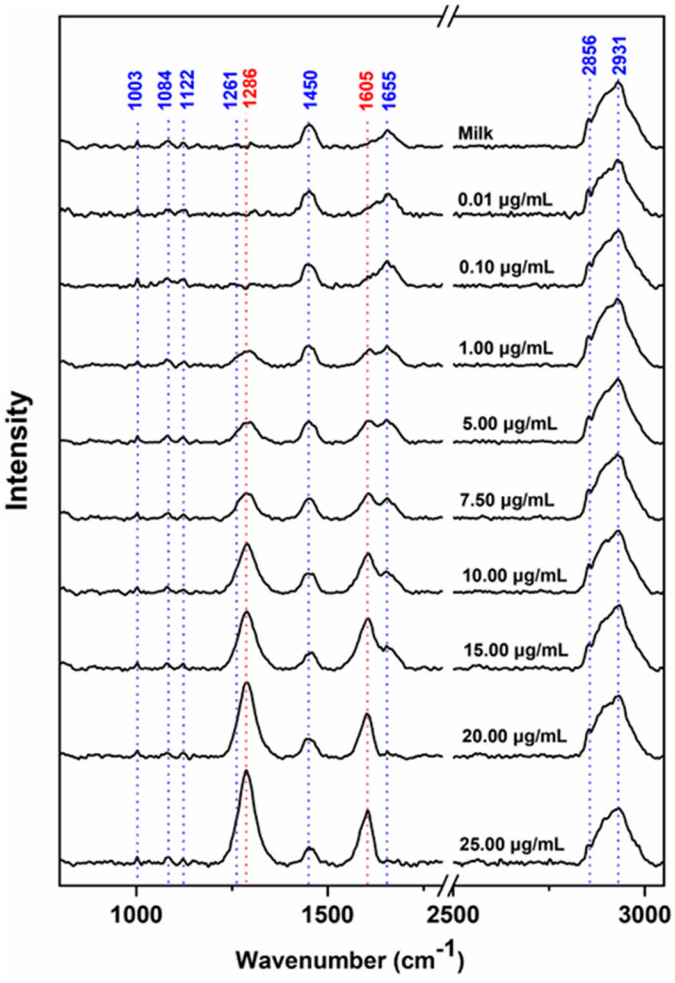

Figure 1. Raman spectra of raw milk (top spectrum) and multi-walled carbon nanotube (MWCNT) dispersions in milk, in concentrations from 0.01 to 25.00 µg/mL. The dotted lines represent the main Raman features observed for milk (blue) and MWCNT (red).

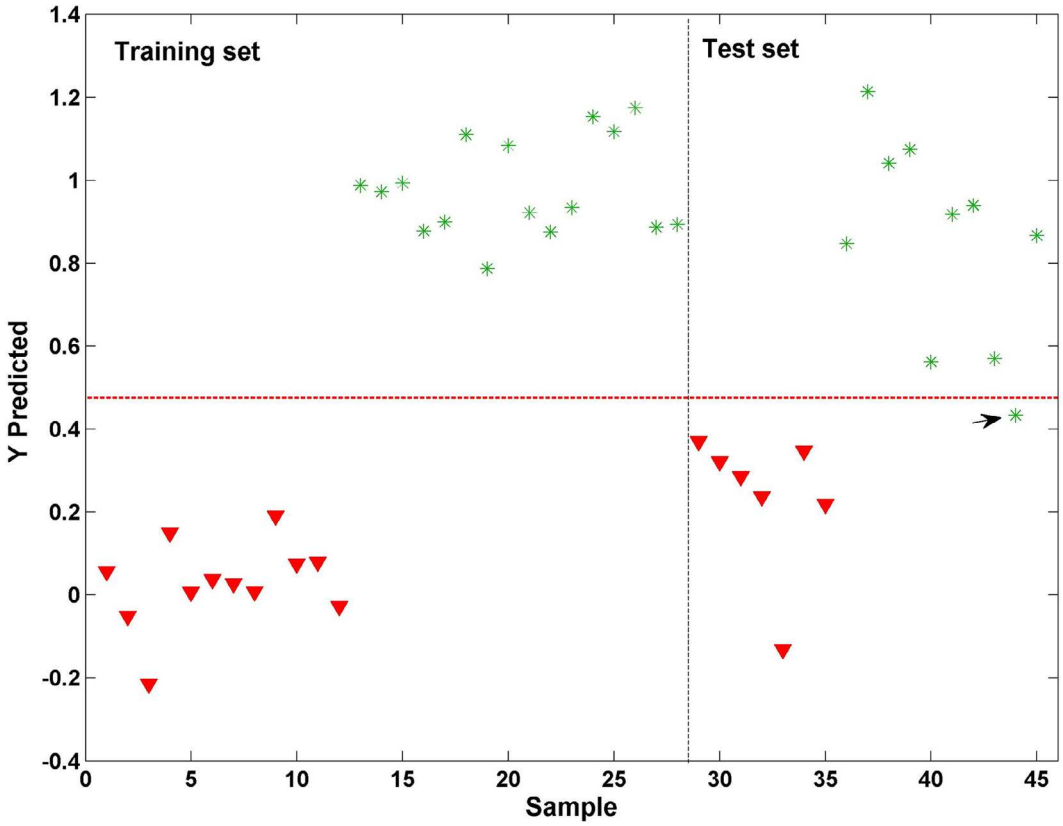

Figure 2. Results of the training and test sets of the partial least squares for discriminant analysis (PLS-DA) model, showing positive multiwalled carbon nanotube (MWCNT) milk samples (asterisks) and milk samples (triangles). The black arrow indicates the only false-negative sample of the test set, with 0.01 μg/mL MWCNT. Sensitivity was 100% and 90%, specificity was 100% and 100%, and efficiency was 100% and 90% for training and test sets, respectively.

The Raman spectrum of milk observed in this study agrees with studies that used liquid cow milk (El-Abassy et al., 2011) and whole milk powder (Almeida et al., 2011; Rodrigues Júnior et al., 2016). The bands at 2,931 and 2,856 cm^{-1} are related to the asymmetric (ν_{ass}) and symmetric (ν_s) CH_2 stretching modes, respectively. The stretch (C-H) is related to the fatty acids content in milk, and the prominent intensity of the symmetric CH_2 stretch band at 2,853 cm^{-1} are characteristic of milk with higher fat content. The band at 1,655 cm^{-1} corresponds to association between ν(C = O) stretching of amide I mode from milk proteins and ν(C = C) *cis* double-bond stretching from the UFA. The band observed at 1,450 cm^{-1} are correlated with the carbohydrate content of milk and represents the $\delta(CH_2)$ scissoring CH_2 deformation. The bands observed in milk under 1,280 cm^{-1} are related to carbohydrates. The band at 1,261 cm^{-1} correspond to the $\gamma(CH_2)$ twisting mode, and 1,122 to 1,082 cm^{-1} correspond to associations between ν(C-O) and ν(C-C) stretching modes and γ(C-O-H) twisting modes. The band observed at 1,003 cm^{-1} is related to the ring-breathing mode of the phenylalanine AA present in milk. The weak and unidentified bands under 1,000 cm^{-1} are related to δ(C-O-C) and δ(C-C-O) scissoring modes and the presence of glucose and lactose (Almeida et al., 2011; El-Abassy et al., 2011; Rodrigues Júnior et al., 2016).

The MWCNT has vibrational characteristics that can also be assessed by Raman scattering spectroscopy. Beyond milk scattering bands, the 2 most important bands in the spectrum of milk samples with MWCNT are identified in 1,605 and 1,286 cm^{-1} wavelengths. The first represents the G band, resulted from the ν(C = C) tangential stretching modes of the MWCNT (Jorio et al., 2004; Bokobza and Zhang, 2012). The second one represents the D band, resulted from the aromatic ring-breathing modes of the MWCNT, induced by disorders on the hexagonal lattice. This D scattering band is also induced by surface modifications due to the addition of carboxylic and phenolic functional groups over MWCNT during oxidation process (Sato et al., 2005; Sekar et al., 2015).

A PLS-DA model was built to identify the presence of MWCNT in milk samples, especially at low concentrations, because at higher concentrations, visual detection is possible. As previously described in

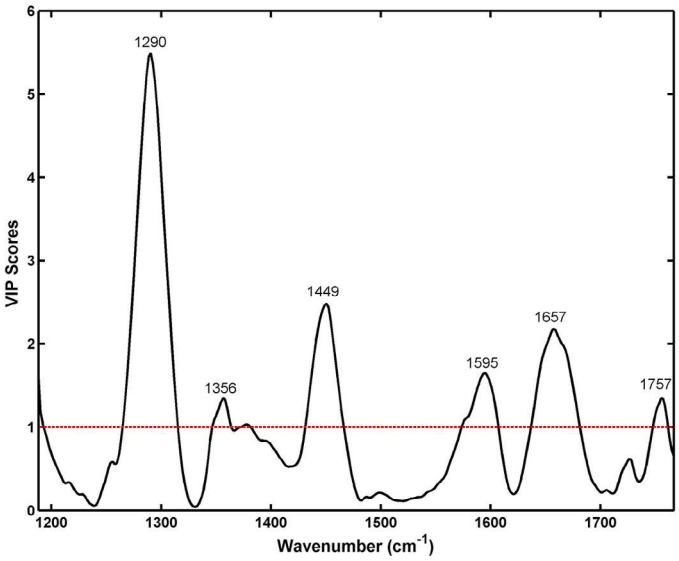

Figure 3. Variable importance in projection (VIP) scores (black line) for the spectral characterization of the partial least squares for discriminant analysis model developed using spectra from different multi-walled carbon nanotube dilutions in milk samples. The horizontal dotted line indicates the threshold of 1.0, above which variables are considered important to the overall model performance.

the "Material and Methods" section, the model was constructed using 28 samples with 5 LV, accounting for 97.6% and 95.1% of the total variance in the **X** matrix and **Y** vector, respectively. The number of LV was selected according to the smallest misclassification in cross-validation, as shown in Supplemental Figure S3 (http://osf.io/s5eq6; Nunes, 2023). The model with 5 LV showed a sensitivity of 100%, specificity of 93.8%, and a classification error rate of 3.1% during cross-validation. Figure 2 shows the PLS-DA predictions for the training and test sets. The Bayesian threshold was calculated as 0.476; milk samples below this value were classified as MWCNT-negative, while those above were classified as MWCNT-positive.

All the training samples were correctly classified by the model, resulting in no false-positive or false-negative classifications (Figure 2). In the test set, only one false-negative result was observed. The misclassified sample had an MWCNT concentration of 0.01 μg/mL, indicating that it is not possible to carry out identification using ordinary Raman spectroscopy for concentrations equal to or less than this value. The PLS-DA model can correctly classify milk samples with up to 0.1 μg/mL MWCNT. However, this exploratory research did not assess the capability of the PLS-DA model to classify milk with dilutions of MWCNT between 0.09 to 0.02 μg/mL; this requires more investigation.

The figures of merit were calculated to demonstrate the ability of the PLS-DA model in detecting milk samples with MWCNT. The sensitivity was 100% and 90% for the training and test sets, respectively. The specificity was 100% for the training and test sets, and the efficiency rate was estimated to be 100% for the training set and 90% for the test set. These results are summarized in Table 1.

For the spectral characterization of the developed model, it is interesting to observe the VIP scores shown in Figure 3. Variables with VIP scores higher than 1.0 are considered to contribute significantly to the detection of milk samples containing MWCNT in the model. Analysis of these scores reveal that the D band (1,290 cm^{-1}) is the highest contributor. The remaining notable VIP score bands (1,356, 1,449, 1,657, and 1,757 cm^{-1}) are associated with vibrational modes characteristic of milk (Almeida et al., 2011; El-Abassy et al., 2011; Ro-

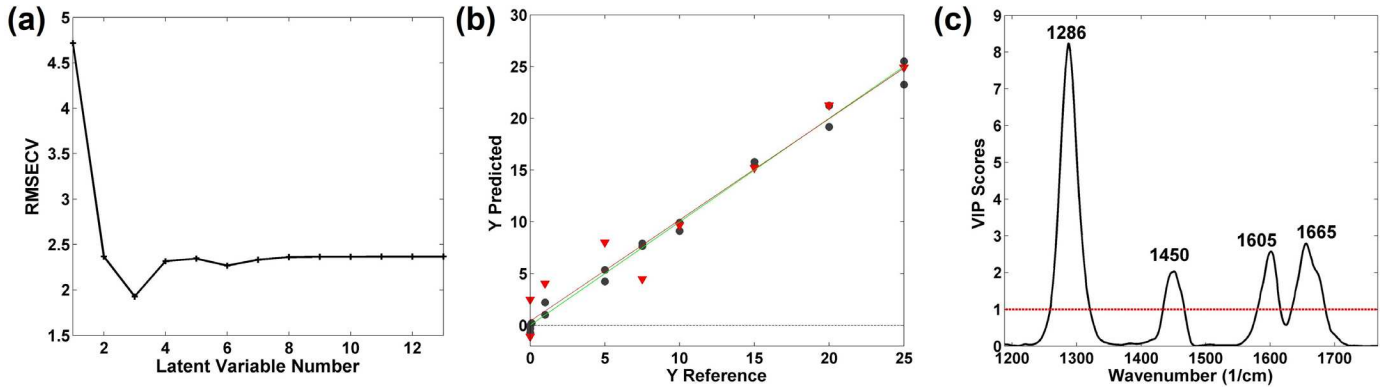

Figure 4. Partial least squares (PLS) models. (a) Variable latent number based in lower root mean square error of cross-validation (RMSECV). (b) Plot of Y reference values versus Y predicted values in the PLS model for multiwalled carbon nanotube concentrations in milk. Black circles indicate calibration samples, and red triangles indicate validation samples. (c) Variable importance in projection (VIP) scores showing the Raman band contribution for the PLS model.

Table 2. Parameters and results for the developed partial least squares model to predict the amount of multiwalled carbon nanotubes in milk[1]

No. of latent variables	RMSEC (μg/mL)	RMSECV (μg/mL)	RMSEP (μg/mL)	RPD_{cal}	RPD_{val}
3	1.53	1.92	1.99	5.7	4.5

[1]RMSEC = root mean square error of calibration; RMSECV = root mean square error of cross-validation; RMSEP = root mean square error of prediction; RPD_{cal} = residual prediction deviation of calibration; RPD_{val} = residual prediction deviation of validation.

drigues Júnior et al., 2016; Gómez-Mascaraque et al., 2020, Genis et al., 2021). Out of these scores, the second most intense band at 1,449 cm^{-1} may be associated with the carbohydrate and fat content of milk, which represents $\delta(CH_2)$ scissoring CH_2 deformation (Almeida et al., 2011; Gómez-Mascaraque et al., 2020). The third most intense band at ~1,650 cm^{-1} is assigned to the amide I mode from milk proteins (Almeida et al., 2011; Rodrigues Júnior et al., 2016). The Raman band at 1,757 cm^{-1} corresponds to the vibrational mode associated with the presence of fatty acids (C = O stretching ester), and the band at 1,356 cm^{-1} (C-O stretching and C-O-H deformation) is attributed to the presence of carbohydrates in milk samples (Almeida et al., 2011; El-Abassy et al., 2011; Gómez-Mascaraque et al., 2020). Finally, the fourth highest score at 1,595 cm^{-1} represents the G band of MWCNT. To verify a possible interference between MWCNT and milk components, a principal component analysis model was built with only milk samples (without the addition of MWCNT). The contribution of milk Raman bands in VIP scores is due to changes in milk composition from sample to sample, as can be seen in the scores and loadings of the principal component analysis model (Supplemental Figure S4; http://osf.io/s5eq6; Nunes, 2023).

After building the classification model to detect the presence of MWCNT in milk samples, a regression model was built to predict the amount of MWCNT. The PLS model was built with 3 LV, and the number of LV was selected according to the smallest RMSECV (1.92 μg/mL), as shown in Figure 4a. The results for the PLS model, including RMSEC, RMSEP, and RPD, are shown in Table 2. The accuracy of the model can be evaluated by RMSEC and RMSEP, which for the model built are 1.53 and 1.99 μg/mL, respectively. The prevision relative errors are lower than 18%, and for samples with low concentrations, the relative error was greater. Another parameter evaluated in the model was the RPD (Williams, 2001). Models with RPD above 2.4 present good predictive ability. The PLS model presented an RPD of 5.7 and 4.5 for the calibration and validation sets, respectively. Figure 4b shows a plot of the MWCNT content predicted by the PLS model. The calibration set shows a correlation of 0.968, whereas the validation samples showed a correlation of 0.975. As in the PLS-DA model, the informative vectors were analyzed to characterize the model and the VIP scores are shown in Figure 4c. The identification of the spectral regions that contribute more to predicting the MWCNT content was possible. As it was expected, the D band at 1,286 cm^{-1} is the main contribution to the quantification model. The other MWCNT band at 1,605 cm^{-1} also contributes to the model, just like the 1,450 and 1,665 cm^{-1} milk bands. The results obtained in this work show the potential of Raman spectroscopy for detecting and quantifying MWCNT in raw milk samples.

CONCLUSIONS

This exploratory study proposes a simple and rapid method based on Raman spectroscopy and chemometrics tools to detect and quantify concentrations of MWCNT in cow milk equal to greater than 0.1 μg/mL. The chemometric models were built and validated using a set of test samples and spectrally interpreted based on the highest VIP scores. This allowed the identification of the vibrational modes associated with the D and G bands of MWCNT and characteristic milk bands. This methodology requires more research and has the potential to be implemented by dairy industry as a screening method for detecting carbon nanotubes in milk intended for processing, as a food safety practice while the use of nanomaterials in veterinary medicine is growing.

ACKNOWLEDGMENTS

This work was supported by FAPEMIG (Fundação de Amparo à Pesquisa do Estado de Minas, Brazil; grant number APQ-01591-14). PPN, CF, CAF, LOL, AJV, and RLS have fellowships from CNPq (Conselho Nacional de Desenvolvimento Científico e Tecnológico, Brazil). FGP works as researcher in MG Graphene Project CDTN/UFMG/CODEMGE (Centro de Desenvolvimento da Tecnologia Nuclear/Universidade Federal de Minas Gerais/Companhia de Desenvolvimento Econômico de Minas Gerais, Brazil). RKFGO works as a process technician at CTNano, UFMG (Centro de Tecnologia em Nanomateriais e Grafeno, Universidade Federal de Minas Gerais, Brazil). The authors have not stated any conflicts of interest.

REFERENCES

Ali-Boucetta, H., and K. Kostarelos. 2013. Pharmacology of carbon nanotubes: Toxicokinetics, excretion and tissue accumulation. Adv. Drug Deliv. Rev. 65:2111–2119. https://doi.org/10.1016/j.addr.2013.10.004.

Almeida, M. R., K. S. Oliveira, R. Stephani, and L. F. C. de Oliveira. 2011. Fourier-transform Raman analysis of milk powder: A potential method for rapid quality screening. J. Raman Spectrosc. 42:1548–1552. https://doi.org/10.1002/jrs.2893.

Almeida, M. R., K. S. Oliveira, R. Stephani, and L. F. C. de Oliveira. 2012. Application of FT-Raman spectroscopy and chemometric analysis for determination of adulteration in milk powder. Anal. Lett. 45:2589–2602. https://doi.org/10.1080/00032719.2012.698672.

Apartsin, E. K., M. Y. Buyanova, D. S. Novopashina, E. I. Ryabchikova, A. V. Filatov, M. A. Zenkova, and A. G. Venyaminova. 2014. Novel multifunctional hybrids of single-walled carbono nanotubes with nucleic acids: Synthesis and interactions with living cells. ACS Appl. Mater. Interfaces 6:1454–1461. https://doi.org/10.1021/am4034729.

Bando, E., R. C. Oliveira, G. M. Z. Ferreira, and M. Machinski Jr.. 2009. Occurrence of antimicrobial residues in pasteurized milk commercialized in the state of Paraná, Brazil. J. Food Prot. 72:911–914. https://doi.org/10.4315/0362-028X-72.4.911.

Barkalina, N., C. Jones, J. Kashir, S. Coote, X. Huang, R. Morrison, H. Townley, and K. Coward. 2014. Effects of mesoporous silica nanoparticles upon the function of mammalian sperm in vitro. Nanomedicine 10:859–870. https://doi.org/10.1016/j.nano.2013.10.011.

Bianco, A., K. Kostarelos, C. D. Partidos, and M. Prato. 2005. Biomedical applications of functionalized carbon nanotubes. Chem. Commun. (Camb.) 5:571–577. https://doi.org/10.1039/b410943k.

Bokobza, L., and J. Zhang. 2012. Raman spectroscopic characterization of multiwall carbon nanotubes and of composites. Express Polym. Lett. 6:601–608. https://doi.org/10.3144/expresspolymlett.2012.63.

Bottini, M., S. Bruckner, K. Nika, N. Bottini, S. Bellucci, A. Magrini, A. Bergamaschi, and T. Mustelin. 2006. Multi-walled carbon nanotubes induce T-lymphocyte apoptosis. Toxicol. Lett. 160:121–126. https://doi.org/10.1016/j.toxlet.2005.06.020.

Chaudhury, K., N. Babu K, A. K. Singh, S. Das, A. Kumar, and S. Seal. 2013. Mitigation of endometriosis using regenerative cerium oxide nanoparticles. Nanomedicine 9:439–448. https://doi.org/10.1016/j.nano.2012.08.001.

Chen, J., G. Ying, and W. Deng. 2019. Antibiotic residues in food: Extraction, analysis, and human health concerns. J. Agric. Food Chem. 67:7569–7586. https://doi.org/10.1021/acs.jafc.9b01334.

Dal Bosco, L., G. E. Weber, G. M. Parfitt, A. P. Cordeiro, S. K. Sahoo, C. Fantini, M. C. Klosterhoff, L. A. Romano, C. A. Furtado, A. P. Santos, J. M. Monserrat, and D. M. Barros. 2015. Biopersistence of PEGylated carbon nanotubes promotes a delayed antioxidant response after infusion into the rat hippocampus. PLoS One 10:e0129156. https://doi.org/10.1371/journal.pone.0129156.

Das, K. K., L. Bancroft, X. Wang, J. C. Chow, B. Xing, and Y. Yang. 2018a. Digestion coupled with programmed thermal analysis for quantification of multiwall carbon nanotubes in plant tissues. Environ. Sci. Technol. Lett. 5:442–447. https://doi.org/10.1021/acs.estlett.8b00287.

Das, K. K., Y. You, M. Torres, F. Barrios-Masias, X. Wang, S. Tao, B. Xing, and Y. Yang. 2018b. Development and application of a digestion-Raman analysis approach for studying multiwall carbon nanotube uptake in lettuce. Environ. Sci. Nano 5:659–668. https://doi.org/10.1039/C7EN01047H.

de Sá Oliveira, K. S., L. S. Callegaro, R. Stephani, M. R. Almeida, and L. F. C. de Oliveira. 2016. Analysis of spreadable cheese by Raman spectroscopy and chemometric tools. Food Chem. 194:441–446. https://doi.org/10.1016/j.foodchem.2015.08.039.

El-Abassy, R. M., P. J. Eravuchira, P. Donfack, B. Von der Kammer, and A. Materny. 2011. Fast determination of milk fat content using Raman spectroscopy. Vib. Spectrosc. 56:3–8. https://doi.org/10.1016/j.vibspec.2010.07.001.

Firme, C. P. III, and P. R. Bandaru. 2010. Toxicity issues in the application of carbon nanotubes to biological systems. Nanomedicine 6:245–256. https://doi.org/10.1016/j.nano.2009.07.003.

Genis, D. O., B. Sezer, S. Durna, and I. H. Boyaci. 2021. Determination of milk fat authenticity in ultra-filtered white cheese by using Raman spectroscopy with multivariate data analysis. Food Chem. 336:127699. https://doi.org/10.1016/j.foodchem.2020.127699.

Girardi, F. A., G. E. Bruch, C. S. Peixoto, L. Dal Bosco, S. K. Sahoo, C. O. F. Gonçalves, A. P. Santos, C. A. Furtado, C. Fantini, and D. M. Barros. 2017. Toxicity of single-wall carbon nanotubes functionalized with polyethylene glycol in zebrafish (*Danio rerio*) embryos. J. Appl. Toxicol. 37:214–221. https://doi.org/10.1002/jat.3346.

Gómez-Mascaraque, L. G., K. Kilcawley, D. Hennessy, J. T. Tobin, and T. F. O'Callaghan. 2020. Raman spectroscopy: A rapid method to assess the effects of pasture feeding on the nutritional quality of butter. J. Dairy Sci. 103:8721–8731. https://doi.org/10.3168/jds.2020-18716.

Ijima, S. 1991. Helical microtubules of graphitic carbon. Nature 354:56–58. https://doi.org/10.1038/354056a0.

Jacobsen, N. R., P. Moller, P. A. Clausen, A. T. Saber, C. Micheletti, K. A. Jensen, H. Wallin, and U. Vogel. 2017. Biodistribution of carbon nanotubes in animal models. Basic Clin. Pharmacol. Toxicol. 121(S3):30–43. https://doi.org/10.1111/bcpt.12705.

Jorio, A., R. Saito, G. Dresselhaus, and M. S. Dresselhaus. 2004. Determination of nanotubes properties by Raman spectroscopy. Philos. Trans. A Math. Phys. Eng. Sci. 362:2311–2336. https://doi.org/10.1098/rsta.2004.1443.

Kennard, R. W., and L. A. Stone. 1969. Computer aided design of experiments. Technometrics 11:137–148. https://doi.org/10.1080/00401706.1969.10490666.

Ladeira, M. S., V. A. Andrade, E. R. M. Gomes, C. J. Aguiar, E. R. Moraes, J. S. Soares, E. E. Silva, R. G. Lacerda, L. O. Ladeira, A. Jorio, P. Lima, M. Fatima Leite, R. R. Resende, and S. Guatimosim. 2010. Highly efficient siRNA delivery system into human and murine cells using single-wall carbon nanotubes. Nanotechnology 21:385101. https://doi.org/10.1088/0957-4484/21/38/385101.

Lee, N. H., S. H. Nahm, and I. S. Choi. 2018. Real-time monitoring of a botulinum neurotoxin using all-carbon nanotube-based field-effect transistor devices. Sensors (Basel) 18:4235. https://doi.org/10.3390/s18124235.

Lekshmi, G., S. S. Sana, V. H. Nguyen, T. H. C. Nguyen, C. C. Nguyen, Q. V. Le, and W. Peng. 2020. Recent progress in carbon nanotube polymer composites in tissue engineering and regeneration. Int. J. Mol. Sci. 21:6440. https://doi.org/10.3390/ijms21176440.

Linn, J. G. 1988. Factors affecting the composition of milk from dairy cows. Pages 224–241 in National Research Council (US) Committee on Technological Options to Improve the Nutritional Attributes of Animal Products. Designing Foods: Animal Product Options in the Marketplace. National Academies Press. Accessed May 10, 2023. https://www.ncbi.nlm.nih.gov/books/NBK218193/.

Liu, Z., K. Chen, C. Davis, S. Sherlock, Q. Cao, X. Chen, and H. Dai. 2008. Drug delivery with carbon nanotubes for in vivo cancer treatment. Cancer Res. 68:6652–6660. https://doi.org/10.1158/0008-5472.CAN-08-1468.

Mazurek, S., R. Szostak, T. Czaja, and A. Zachwieja. 2015. Analysis of milk by FT-Raman spectroscopy. Talanta 138:285–289. https://doi.org/10.1016/j.talanta.2015.03.024.

Munk, M., L. S. A. Camargo, C. C. R. Quintão, S. R. Silva, E. D. Souza, N. R. B. Raposo, J. M. Marconcini, A. Jorio, L. O. Ladeira, and H. M. Brandão. 2016. Biocompatibility assessment of fibrous nanomaterials in mammalian embryos. Nanomedicine 12:1151–1159. https://doi.org/10.1016/j.nano.2016.01.006.

Newman, P., A. Minett, R. Ellis-Behnke, and H. Zreiqat. 2013. Carbon nanotubes: Their potential and pitfalls for bone tissue regeneration and engineering. Nanomedicine 9:1139–1158. https://doi.org/10.1016/j.nano.2013.06.001.

Nunes, K. M., M. V. O. Andrade, M. R. Almeida, and M. M. Sena. 2020. A soft discriminant model based on mid-infrared spectra of bovine meat purges to detect economic motivated adulteration

by the addition of non-meat ingredients. Food Anal. Methods 13:1699–1709. https://doi.org/10.1007/s12161-020-01795-3.

Nunes, P. P. 2023. Nunes et al., JDS support information. http://osf.io/s5eq6.

Pacheco, F. G., A. A. C. Cotta, H. F. Gorgulho, A. P. Santos, W. A. A. Macedo, and C. A. Furtado. 2015. Comparative temporal analysis of multiwalled carbon nanotube oxidation reactions: evaluating chemical modifications on true nanotube surface. Appl. Surf. Sci. 357:1015–1023. https://doi.org/10.1016/j.apsusc.2015.09.054.

Pantarotto, D., R. Singh, D. McCarthy, M. Erhardt, J. P. Briand, M. Prato, K. Kostarelos, and A. Bianco. 2004. Functionalized carbon nanotubes for plasmid DNA gene delivery. Angew. Chem. Int. Ed. Engl. 43:5242–5246. https://doi.org/10.1002/anie.200460437.

Pourasl, A. H., M. T. Ahmadi, M. Rahmani, H. C. Chin, C. S. Lim, R. Ismail, and M. L. P. Tan. 2014. Analytical modeling of glucose biosensors based on carbon nanotubes. Nanoscale Res. Lett. 9:33. https://doi.org/10.1186/1556-276X-9-33.

Redding, L. E., F. Cubas-Delgado, M. D. Sammel, G. Smith, D. T. Galligan, M. Z. Levy, and S. Hennessy. 2014. Antibiotic residues in milk from small dairy farms in rural Peru. Food Addit. Contam. Part A Chem. Anal. Control Expo. Risk Assess. 31:1001–1008. https://doi.org/10.1080/19440049.2014.905877.

Rodrigues Júnior, P. H., K. D. S. de Sá Oliveira, C. E. R. De Almeida, L. F. C. De Oliveira, R. Stephani, M. D. S. Pinto, A. F. De Carvalho, and I. T. Perrone. 2016. FT-Raman and chemometric tools for rapid determination of quality parameters in milk powder: Classification of samples for the presence of lactose and fraud detection by addition of maltodextrin. Food Chem. 196:584–588. https://doi.org/10.1016/j.foodchem.2015.09.055.

Rodriguez-Yañez, Y., B. Muñoz, and A. Albores. 2013. Mechanisms of toxicity by carbono nanotubes. Toxicol. Mech. Methods 23:178–195. https://doi.org/10.3109/15376516.2012.754534.

Sato, Y., A. Yokoyama, K. Shibata, Y. Akimoto, S. Ogino, Y. Nodasaka, T. Kohgo, K. Tamura, T. Akasaka, M. Uo, K. Motomiya, B. Jeyadevan, M. Ishiguro, R. Hatakeyama, F. Watari, and K. Tohji. 2005. Influence of length on cytotoxicity of multi-walled carbon nanotubes against human acute monocytic leukemia cell line THP-1 in vitro and subcutaneous tissue of rats in vivo. Mol. Biosyst. 1:176–182. https://doi.org/10.1039/b502429c.

Sekar, G., S. T. Kandiyil, A. Sivakumar, A. Mukherjee, and N. Chandrasekaran. 2015. Binding studies of hydroxylated multi-walled carbon nanotubes to hemoglobin, gamma globulin and transferrin. J. Photochem. Photobiol. B 153:222–232. https://doi.org/10.1016/j.jphotobiol.2015.09.023.

Shimizu, M., Y. Kobayashi, T. Mizoguchi, H. Nakamura, I. Kawahara, N. Narita, Y. Usui, K. Aoki, K. Hara, H. Haniu, N. Ogihara, N. Ishigaki, K. Nakamura, H. Kato, M. Kawakubo, Y. Dohi, S. Taruta, Y. A. Kim, M. Endo, H. Ozawa, N. Udagawa, N. Takahashi, and N. Saito. 2012. Carbon nanotubes induce bone calcification by bidirectional interaction with osteoblasts. Adv. Mater. 24:2176–2185. https://doi.org/10.1002/adma.201103832.

Singh, R., D. Pantarotto, L. Lacerda, G. Pastorin, C. Klumpp, M. Prato, A. Bionco, and K. Kostarelos. 2006. Tissue biodistribution and blood clearance rates of intravenously administered carbon nanotube radiotracers. Proc. Natl. Acad. Sci. USA 103:3357–3362. https://doi.org/10.1073/pnas.0509009103.

Tempini, P. N., S. S. Aly, B. M. Karle, and R. V. Pereira. 2018. Multidrug residues and antimicrobial resistance patterns in waste milk from dairy farms in central California. J. Dairy Sci. 101:8110–8122. https://doi.org/10.3168/jds.2018-14398.

Varkouhi, A. K., S. Foillard, T. Lammers, R. M. Schiffelers, E. Doris, W. E. Hennink, and G. Storm. 2011. SiRNA delivery with functionalized carbon nanotubes. Int. J. Pharm. 416:419–425. https://doi.org/10.1016/j.ijpharm.2011.02.009.

Williams, P. C. 2001. Implementation of near-infrared technology. Pages 1345–169 in Near-infrared Technology in the Agricultural and Food Industries. P. C. Williams and K. Norris, ed. American Association of Cereal Chemists.